

The C-start escape response of *Polypterus senegalus*: bilateral muscle activity and variation during stage 1 and 2

Eric D. Tytell* and George V. Lauder†

Department of Organismic and Evolutionary Biology, Harvard University, Cambridge, MA 02138, USA

e-mail: *tytell@oeb.harvard.edu and †glauder@oeb.harvard.edu

Accepted 30 May 2002

Summary

The fast-start escape response is the primary reflexive escape mechanism in a wide phylogenetic range of fishes. To add detail to previously reported novel muscle activity patterns during the escape response of the bichir, *Polypterus*, we analyzed escape kinematics and muscle activity patterns in *Polypterus senegalus* using high-speed video and electromyography (EMG). Five fish were filmed at 250 Hz while synchronously recording white muscle activity at five sites on both sides of the body simultaneously (10 sites in total). Body wave speed and center of mass velocity, acceleration and curvature were calculated from digitized outlines. Six EMG variables per channel were also measured to characterize the motor pattern. *P. senegalus* shows a wide range of activity patterns, from very strong responses, in which the head often touched the tail, to very weak responses. This variation in strength is significantly correlated with the

stimulus and is mechanically driven by changes in stage 1 muscle activity duration. Besides these changes in duration, the stage 1 muscle activity is unusual because it has strong bilateral activity, although the observed contralateral activity is significantly weaker and shorter in duration than ipsilateral activity. Bilateral activity may stiffen the body, but it does so by a constant amount over the variation we observed; therefore, *P. senegalus* does not modulate fast-start wave speed by changing body stiffness. Escape responses almost always have stage 2 contralateral muscle activity, often only in the anterior third of the body. The magnitude of the stage 2 activity is the primary predictor of final escape velocity.

Key words: fast-start, fish, kinematics, electromyography, bichir, *Polypterus senegalus*, bilateral activity, body stiffness.

Introduction

Many fishes display a classic C-start escape response when startled. Because this response is a major predator avoidance behavior for many fishes, it often involves near maximal performance. The neural control mechanism underlying C-starts is also relatively well understood. As such, the escape response provides a useful system for studying locomotor performance and neurobiology in fishes. Kinematics (reviewed in Domenici and Blake, 1997), muscle activity patterns (Jayne and Lauder, 1993; Westneat et al., 1998; Ellerby and Altringham, 2001) and neurobiology (Eaton et al., 1988, 1991; Fetcho, 1991) have been studied in a diverse phylogenetic range of fishes (Hale et al., 2002).

Typically, an escape response consists of two stages (Weihs, 1972). Stage 1, the 'preparatory' stage, involves a tight bend to one side, causing a C-shaped curve in the body. The ipsilateral (concave) side usually has strong muscle activity, whereas muscle activity on the contralateral (convex) side is usually inhibited. This stage is typically initiated by a pair of large medullary neurons, called Mauthner cells, that stimulate simultaneous muscle activity down the opposite sides of the body. A structure called the axon cap prevents both Mauthner cells from firing at the same time, causing a unilateral

contraction that gives the C shape (reviewed in Eaton et al., 1991). Stage 2 is the 'propulsive' stage, involving a wave of muscle activity on the contralateral side, which causes the fish to kick out of the C shape. These divisions are somewhat arbitrary, because body bending varies substantially between responses.

Westneat et al. (1998) observed that the escape response of the marbled bichir, *Polypterus palmas*, has a different muscle activity pattern from the typical one described above. They measured strong muscle activity on both sides of the body during stage 1. Little muscle activity was observed during stage 2, although the propulsive kick that usually accompanies such stage 2 activity was present. They hypothesized that the observed bilateral muscle contraction would increase body stiffness and thus increase the speed of the propulsive body wave. Because they infrequently observed stage 2 muscle activity, they presumed that all the force for the stage 2 kick must come from passive straightening of the body. However, their study focused on intramuscular pressure, and had fewer EMG recording sites and experiments than the current study. While their data clearly show the presence of stage 1 bilateral activity, further detail will help to characterize its longitudinal

extent, variability, and, in the end, its function. Additional information on stage 2 activity, particularly in the anterior body, should clarify the relative importance of muscle activity and passive straightening during stage 2.

In this study, we characterize the novel escape response of *Polypterus senegalus* in detail. We focus on the frequency and longitudinal extent of stage 1 bilateral activity and stage 2 contralateral activity and both their functional consequences and describe the substantial and previously undocumented variability in escape response performance. Electromyographic (EMG) recordings were obtained at five sites on both sides of the body to quantify the variation in contralateral activity during stage 1 and to determine the presence or absence of stage 2 activity. These recordings were correlated with simultaneously recorded midline kinematics to test the effect of the previously reported novel muscle activation pattern on escape response performance. A large number of recordings were essential to discern specific effects through the variation in the data. Specifically, we examined the association between contralateral muscle activity, body stiffness, bending wave speed, and overall escape performance, as well as the role of stage 2 muscle activity.

Additionally, our detailed characterization of the novel muscle activation pattern in the escape response of *Polypterus* could provide a useful evolutionary comparison. Escape responses have been observed and described over a wide phylogenetic range of fishes (Currie and Carlsen, 1987; Nissanov and Eaton, 1989; Eaton and Emberley, 1991; Jayne and Lauder, 1993; Westneat et al., 1998; Zottoli et al., 1999; Hale et al., 2002). Lamprey (*Petromyzon marinus*) have a different Mauthner cell structure from actinopterygians and retract their heads when startled, rather than performing a C-start (Currie, 1984; Currie and Carlsen, 1987). The head retraction is caused by simultaneous bilateral muscle activity throughout the entire behavior and along the entire length of the body (Currie and Carlsen, 1987). Actinopterygians, including the goldfish, *Carassius auratus*, and the bluegill sunfish, *Lepomis macrochirus*, perform C-start behaviors and often have a short muscle activity spike on the contralateral side during Stage 1 (Eaton and Emberley, 1991; Jayne and Lauder, 1993; Foreman and Eaton, 1993). Unlike in the lamprey, this contralateral spike has a much shorter duration than the ipsilateral activity and probably represents a combination of true muscle activity and a false signal due to cross talk (Foreman and Eaton, 1993), but which has still been hypothesized to stiffen the body (Foreman and Eaton, 1993). Westneat et al. (1998) observed substantially longer contralateral activity in *Polypterus palmas* and *Amia calva*. Additionally, some derived elongate fishes, including the eel, *Anguilla rostrata*, and the spiny eel, *Mastacembelus siamensis*, also perform head retraction, similar to the lamprey, with simultaneous bilateral activity (A. B. Ward, personal communication). The extent of the differences in escape responses between the lamprey and derived fishes is difficult to quantify without a well characterized representative from an intermediate clade. In a recent comparative study, Hale et al.

(2002) examined the evolution of the escape response and characterized *Petromyzon*, *Polypterus*, *Carassius* and *Lepomis* as having bilateral activity. However, the bilateral activity in derived actinopterygians potentially differs substantially from that in more basal fishes (Westneat et al., 1998), both in duration and apparent function. A more detailed characterization of the function and variation in bilateral muscle activity in *Polypterus*, a basal actinopterygian, will clarify this proposed evolutionary sequence.

Materials and methods

Fish

We obtained bichirs, *Polypterus senegalus* Cuvier, from a local aquarium supplier, and housed the specimens individually in 10 gallon aquaria at 24 ± 1 °C with a 12:12 h light:dark cycle. We performed experiments on 5 individuals, mean total length $L = 16.6 \pm 0.3$ cm (\pm S.E.M.; range 15.7–17.5 cm) and mean mass 24 ± 1 g (\pm S.E.M.; range 22–26 g), in a 25 gallon aquarium (60 cm \times 30 cm). At least 9 escape responses were elicited from each fish by dropping an object (D-cell battery) in the tank near the fish. This type of stimulus has been used in previous studies (Eaton and Emberley, 1991; Jayne and Lauder, 1993) and reliably evoked startle behavior in *P. senegalus*. Care was taken to drop the object from the same height in each experiment and to avoid hitting the fish. The distance between the fish and the stimulus was not controlled; instead the object's position relative to the fish's center of mass at the onset of the response was digitized. The distance between the stimulus and the center of mass and the angle between the snout, center of mass, and the stimulus were then calculated.

A total of 65 C-starts were analyzed. Of these, nine responses had satisfactory EMG recordings but not usable video because the fish was partially out of the field of view, and therefore were included in the analysis of stage 2 activity, but not that of stage 1. Recording a large number of responses was essential to fully characterize the range of variation in the escape response. After each response, fish were allowed to recover for approximately 5 min to avoid habituation to the stimulus. Fish did not show any acclimation or fatigue during the course of the experiment (Fig. 5). After each experiment was complete, the fish were euthanized, weighed and measured. The center of mass was determined by stretching each fish straight on a balanced plastic tray with a fulcrum and adjusting the fish's position until the tray balanced again.

Electromyography

Anesthesia of the fish was induced by approximately 15 min immersion in a buffered 0.03% (by weight) solution of tricaine methane sulfonate (MS222). During surgery, which lasted less than 2 h, anesthesia was maintained by a 0.015% solution of MS222. If opercular pumping ceased, water was pumped over the fish's gills at least every 10 min. All five fish maintained some respiration during surgery. Bipolar electrodes were implanted in epaxial white muscle at five sites on each side of

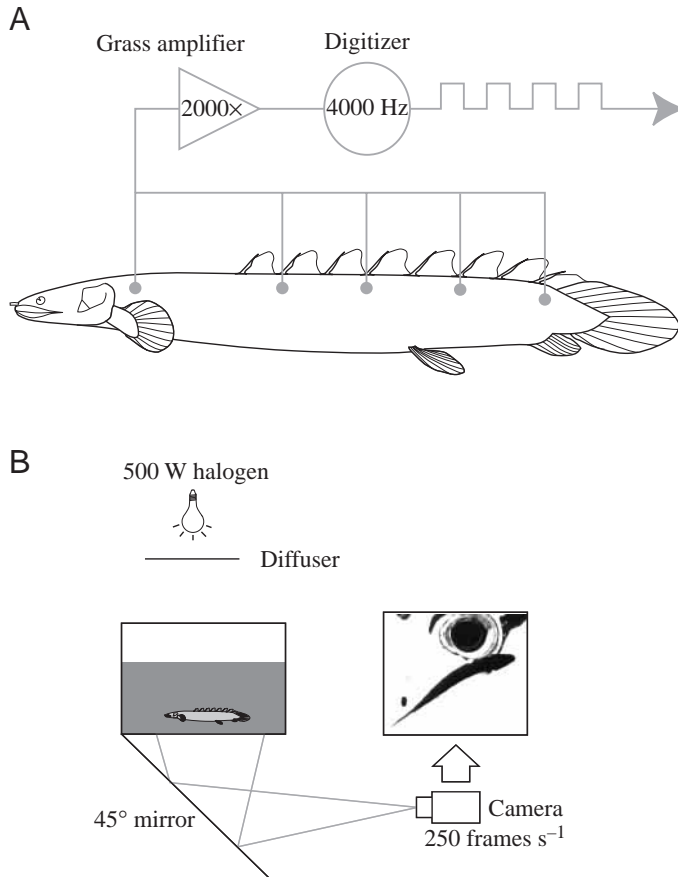


Fig. 1. (A) Diagram of the electromyographic apparatus used to record EMGs, showing longitudinal positions of the electrodes, one on each side of the body. (B) The filming arrangement. A high-speed digital camera filmed a ventral view of the escape responses.

the body: approximately 5 mm posterior to the neurocranium and below fin rays 2, 4, 6 and 9 (Fig. 1), corresponding to positions at 18%, 35%, 46%, 57% and 70% of body length L . We constructed the electrodes by gluing two 2 m lengths of 0.05 mm diameter insulated stainless steel wire together, stripping 0.5 mm of insulation off the ends, and bending the bare ends back to form a hook. The electrodes were implanted using 26 gauge hypodermic needles through 2 mm holes drilled in a scale. After implantation, electrodes were secured individually by filling the drilled holes with cyanoacrylate glue. All ten electrodes were glued together into a cable that was sutured to the second ray, which is close to the center of mass. Ray 1 was removed to avoid entanglement with the wires. Care was taken to ensure each electrode had sufficient slack to allow complete bending of the body without pulling on the implantation site. Each fish was allowed to recover for at least 2 h after surgery. Behavior after surgery was qualitatively unchanged from behavior before surgery. After completion of the experiment, fish were euthanized using an overdose of MS222 and were dissected to confirm positions of the electrodes.

EMG signals were amplified 2000–5000 times using Grass

P511K pre-amplifiers and digitized at 4000 Hz in real time using a PowerLab 16SP analog-to-digital converter (A/D Instruments) and a Micron computer. Signals were initially filtered with a 60 Hz notch filter in the pre-amplifier and later with a high-pass 100 Hz fifth order Butterworth digital filter (Matlab 6.1 and Signal Processing Toolbox 5.1, MathWorks, Inc., Natick, MA, USA).

The timing of muscle activation events was determined using a custom computer program in Matlab, which had four components: (1) estimation of baseline noise levels, (2) rectifying and smoothing, (3) thresholding and elimination of short duration events and (4) manual digitization. First, baseline noise levels were estimated. Because the muscles were active only a small fraction of the total time sampled (approximately 7%), the baseline noise levels were estimated by the interquartile range of the entire sample multiplied by 0.7413. This value provides a robust, unbiased estimate of the standard deviation that ignores outliers (i.e. periods of muscle activity) for the EMG data (Rice, 1995). Second, to determine onset and offset times, the data were rectified and then smoothed using a running median filter of length 2.5 ms (10 samples), which removed transient events shorter than the filter length. This length filter was chosen because it removes transient spikes but retains periods of muscle activity. Note that the median filtered data were only used to determine muscle activity timing, not to calculate activity magnitudes. Third, the smoothed data were thresholded at 20 \times baseline noise level. Because the smoothing blurs the edges of sharp transitions, the initial thresholded values were used to estimate the actual transitions in the unsmoothed data. Any remaining events shorter than the filter length were discarded. Finally, in 5% of events, processing errors required manual digitization. The remaining 95% were not modified. Time $t=0$ was defined as the median ipsilateral onset time for each response.

For each muscle activation event, three values were calculated: onset time, offset time, and magnitude. The magnitude is the integral of the rectified EMG signal, taken with a standard trapezoidal numerical integration routine (Matlab). The voltages from each electrode are not comparable to other voltages directly, and so were normalized by a characteristic voltage CV for that electrode. We defined CV as the average voltage from an electrode during muscle activity in all runs in which that particular electrode was used. Thus, the normalized magnitudes had dimensions of $CV \times \text{time}$.

Kinematic analysis

Ventral views of the fish were recorded at 250 frames s^{-1} using a high-speed digital video system (RedLake) aimed at a front surface mirror below the tank, oriented at 45 $^\circ$ (Fig. 1). Illumination was provided by a 500 W halogen lamp, approximately 1 m above the tank, with a diffuser.

Fish outlines were digitized automatically by a custom Matlab program, which traced and smoothed the outlines of a silhouette of the fish. The tips of the snout and tail were identified manually and a midline was calculated by determining the midpoint of the minimum distance line from

one side of the fish to the other at each point on the body (as in Jayne and Lauder, 1993).

The trajectory of the stretched straight center of mass was used to calculate overall velocity and acceleration, which approximates the position where propulsive forces act (Webb, 1978; Domenici and Blake, 1997). Although the true center of mass will change position as the fish's body bends, the stretched straight center of mass is commonly used and makes our data comparable to previous studies (e.g., Webb, 1983; Domenici and Blake, 1991; Jayne and Lauder, 1993; Foreman and Eaton, 1993; Westneat et al., 1998). Derivatives were calculated using a smoothing spline (Matlab Spline Toolbox 3.0) with mean squared error MSE of 0.5 pixels, the measurement error for any digitized position (MSE routine of Walker, 1998). The angular velocity of the snout with respect to the center of mass was also estimated with a smoothing spline with an error of $\tan^{-1}\sqrt{2MSE/COM}$, the angular error resulting from two independent errors in the position of the snout and the center of mass (Taylor, 1982), where COM is the distance between the snout and the center of mass. Maxima for velocity, acceleration and angular velocity were recorded. The angle of the final trajectory relative to the initial body angle was also recorded. Note that velocity often had two peaks: one during stage 1 and one in stage 2.

The end of stage 1 was defined as the time when the tip of the snout changed its direction of motion, which is equivalent to when the angular velocity changed sign (following Domenici and Blake, 1997). Linear interpolation was used to determine the exact time when the angular velocity was zero. Note that because this definition was based on a kinematic variable, stage 2 muscle activity generally occurred before the end of stage 1 as defined kinematically.

From the midlines, we calculated curvature κ ,

$$\kappa = \frac{\partial x}{\partial s} \frac{\partial^2 y}{\partial s^2} - \frac{\partial y}{\partial s} \frac{\partial^2 x}{\partial s^2}, \quad (1)$$

where x and y are the coordinates of a point on the midline and s is the distance from the tip of the snout to that point along the curve of the midline. Spatial derivatives were calculated with a smoothing spline, as above. The maximum curvature at the center of mass was recorded. Also, the velocity of the body wave was determined by tracking the position of maximum curvature down the body.

Stiffness analysis

Bilateral activation should increase body stiffness, which will increase the body wave speed (Long, 1998). This increase is desirable because body wave speed is often correlated with overall swimming velocity, as well as the swimming efficiency (Lighthill, 1970). To investigate this hypothesis, body wave speed should be regressed against a metric of bilateral activity. A simple physical argument based on static beam loading allows the development of an appropriate metric for the contribution of bilateral activation to stiffening. Consider contraction by both ipsilateral and contralateral muscles, producing forces F_I and F_C , respectively, at a mean distance a

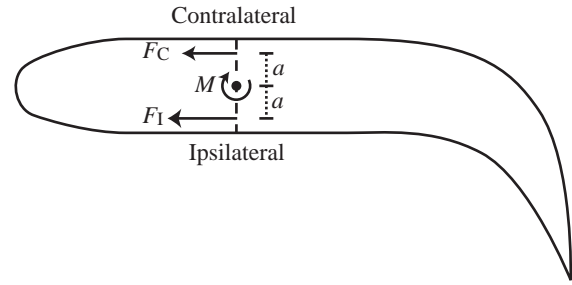


Fig. 2. Diagram of a section of a fish's body with a bending moment M induced by bilateral contraction, with ipsilateral force F_I and contralateral force F_C . Both forces are applied an equal distance a from the midline.

from the midline (Fig. 2). If the total bending moment $M = a(F_I - F_C)$ causes an angular deflection θ of the section, then the flexural stiffness EI is

$$EI = \frac{a(F_I - F_C)L}{\theta}, \quad (2)$$

where L is the length of the section, based on static loading of a homogeneous beam (Beer and Johnston, 1992). The effective flexural stiffness EI_{eff} for the ipsilateral contraction alone is thus increased:

$$\frac{aF_I L}{\theta} = EI_{\text{eff}} = EI + \frac{aF_C L}{\theta}. \quad (3)$$

To simplify the equation for the effective stiffness, we can solve for θ in equation 2, based on the original stiffness, and substitute into equation 3, giving

$$EI_{\text{eff}} = EI \left(1 + \frac{F_C}{F_I - F_C} \right). \quad (4)$$

Therefore, we define the metric B for the relative stiffness of a fish with bilateral muscle activity as

$$B = 1 + \frac{F_C}{F_I - F_C}. \quad (5)$$

In this study, muscle forces were not quantified directly. Therefore, to estimate B , we used parameters of the EMGs, including magnitude and duration, as estimates of force. EMGs, however, do not reflect well the true muscular force (Loeb and Gans, 1986). The estimate of the B parameter based on the EMGs should therefore be considered only a rough estimate of the true relative stiffness. To emphasize this approximation, we use the symbol B_{EMG} for B calculated from EMG data.

Statistics

All statistics were performed using Systat 9.01 (SPSS, Chicago, IL, USA). Initially, a principal components analysis (PCA; see, for example, Dunteman, 1989) was performed on the kinematic data. All eight measured kinematic variables (max. velocity, max. stage 1 velocity, max. acceleration, max. angular velocity, max. curvature, body wave velocity, stage 1

duration, and final trajectory angle) were used in the analysis, which allowed us to reduce the kinematic data set to two variables that captured a large amount of the total variance. Additionally, the PCA allowed a metric of a response's kinematic strength to be generated.

For the stage 1 electromyographic data, we tested the significance of differences in longitudinal position, side of the body (i.e. ipsilateral *versus* contralateral), and kinematic strength, and controlled for the effect of differences in individuals using a four-way mixed-model multivariate analysis of variance (MANOVA) on onset time, offset time and magnitude. Individuals were treated as random effects; all other factors were treated as fixed. Using the guidelines from Zar (1999), the appropriate error terms were calculated: for any fixed effect or interaction between fixed effects, the error term is the interaction between the random effect and the effect or interaction itself. Only interaction terms between fixed effects were tested for significance. The random effect interactions represent inter-individual variation, which was not relevant to this study. After a significant result in the MANOVA, univariate ANOVAs were performed on each of the three variables. For these tests, each channel in each experiment is a separate observation, giving total N values of at least 560. When a particular channel had no muscle activity during a response, we assigned that data point a zero for magnitude and a missing value for onset and offset time. Therefore, the N values for tests on onset and offset were lower (527) than those for magnitude (560). Paired comparisons were conducted using a strict Bonferroni significance level adjustment.

To test the presence of stage 2 activity, a chi-squared test was performed on the frequencies of different numbers of active channels. This test was used to test both homogeneity, or whether the probabilities of the presence or absence of stage 2 activity are equal, and also independence, or whether the probabilities for stage 2 activity vary with some other variable.

All mean values are reported \pm S.E.M.

Results

Substantial variation was observed in the kinematic and electromyographic strengths of the escape responses, ranging from very leisurely turns with short duration EMGs to very rapid turns, in which the head touched the tail and EMGs had a longer duration and greater magnitude. Because of the large number of responses analyzed, statistical tests show, even with this variation, that stage 1 ipsilateral muscle activity is significantly longer, stronger, and starts earlier than contralateral activity. Also, almost all responses had stage 2 muscle activity. In the sections below we detail the range of variation and the methods used to control for it, and present an analysis of stage 1 and 2 muscle activation patterns and their kinematic consequences.

Variation

P. senegalus is capable of escape responses with a wide variation in kinematic strength. Fig. 3 shows examples of

typical EMGs and video frames from a 'strong' and 'weak' escape response. In general, the duration of muscle activity in weak responses was substantially less than those in strong ones. Additionally, maximum curvature, final velocity and acceleration tended to be lower in weak behaviors.

To quantify the variation and, ultimately, the kinematic strength of the responses, we performed principal components analyses (PCAs) on the kinematic variables (Table 1). This analysis also allowed an objective measure of C-start strength to be generated. A plot of the component loadings and scores for the first two components are shown in Fig. 4. These two components, representing 65% of the total variation, were saved according to Kaiser's criterion (Kaiser, 1960). Because the variances represented by PC₁ and PC₂ were approximately equal (36% and 29%, respectively), we chose a C-start strength metric S that weighted each component equally: $S=PC_1-PC_2$. The S value is the distance of any point from the line in Fig. 4; positive values indicate strong responses and negative values indicate weak ones.

No behaviors were obstructed by the aquarium walls. The mean stage 1 duration was 61 ± 2 ms; during this time, fish traveled an average of 19.5 ± 0.9 mm. In an obstructed behavior, the animals would start the behavior closer to the walls than this distance plus one standard deviation (Eaton and Emberley, 1991). All behaviors started more than 33 mm away from the wall (mean distance 103 ± 3 mm) and thus none were classified as obstructed.

Variation did not result from habituation to the stimulus. No kinematic variable showed a significant trend over the duration of the experiments. As an example, Fig. 5 shows the lack of trend for maximum velocity ($P=0.859$); kinematic strength S also showed no trend ($P=0.938$).

The position of the stimulus affects both maximum velocity and final turning angle. Fig. 6A shows the regression of maximum velocity on distance between the stimulus and the fish's center of mass ($P<0.001$; Table 2). Although this regression is significant, the correlation is poor ($r^2=0.227$). No other kinematic variable correlated significantly with the stimulus distance. The angle of the stimulus relative to the initial body angle does not affect velocity, but it does correlate

Table 1. Mean values and timing for kinematic variables

Variable	Mean	Time (ms)
Max. velocity ($L s^{-1}$)	7.6 ± 0.3	84 ± 4
Max. stage 1 velocity ($L s^{-1}$)	6.1 ± 0.2	48 ± 2
Max. acceleration ($L s^{-2}$)	172 ± 8	22 ± 2
Max. curvature (L^{-1})	6.4 ± 0.1	46 ± 1
Max. angular velocity ($rad s^{-1}$)	63 ± 2	31 ± 1
Wave velocity ($L s^{-1}$)	12.2 ± 0.6	
Stage 1 duration (ms)	61 ± 2	
Final trajectory angle ($^\circ$)	130 ± 7	

Values are means \pm S.E.M.

Times are given where appropriate.

Curvature and angular velocity are absolute values.

with the final trajectory angle ($P=0.001$; Table 2). Because the regression coefficient is not significantly different from 1 ($P>0.05$), the mean angular distance between the stimulus and the final trajectory is constant. Thus, the fish is simply turning $169\pm 6^\circ$ away from the stimulus (Fig. 6B), a value that is significantly different from 180° ($t_{55}=1.84$, $P=0.036$).

These changes in kinematics seem to be controlled mechanically by changes in the muscle activity pattern. For example, the maximum velocity achieved during stage 1 is significantly related to the ipsilateral muscle activation

magnitude ($P=0.001$; Fig. 7 and Table 2), although other factors probably contribute, because the correlation between magnitude and velocity is relatively low ($r^2=0.201$).

Stage 1

The relative magnitude and timing of muscle activity during stage 1 was investigated using a four-way mixed model MANOVA. This test determines differences in activity onset time, offset time and magnitude from three fixed factors: the side of the activity (i.e. ipsilateral or contralateral), the position

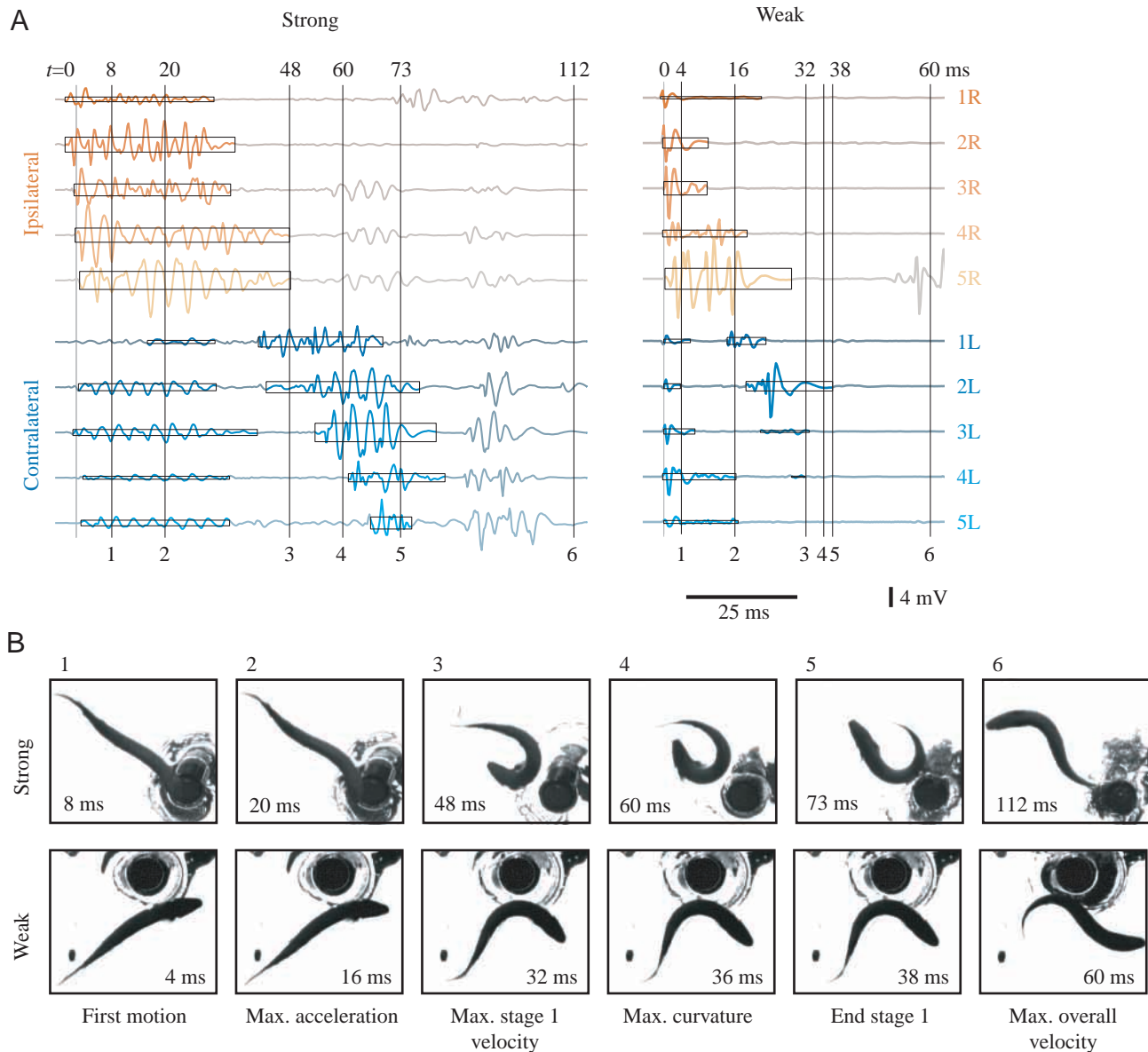


Fig. 3. Typical EMG traces and video frames from strong and weak responses. (A) EMG traces. Traces from ipsilateral and contralateral sites are shown in orange and blue, respectively, and traces from anterior sites are darker than posterior. Periods of escape response muscle activity are shown in a brighter color and are indicated by a box, where the left (L) and right (R) sides signify onset and offset times, respectively, and the height of the box indicates average EMG amplitude. Vertical lines indicate the time of the numbered video frames, shown in B. (B) Video frames corresponding to the same kinematic events in each response. Events shown are (1) first visible motion, usually at the head, (2) maximum acceleration, (3) maximum velocity achieved during stage 1, (4) maximum curvature, (5) end of kinematic stage 1 and (6) maximum overall velocity. Note that the stage 2 muscle activity occurs before the beginning of the kinematic stage 2. Events 4 and 5 (maximum stage 1 velocity and the end of stage 1) for the weak response occur at different times during the same video frame, so that frame is repeated.

Table 2. Regression equations and statistics

Dependent variable	=	Coefficient	×	Independent variable	+	Constant	r^2
Maximum velocity ($L s^{-1}$)	=	-8 ± 2	×	Stimulus distance (L)	+	10.2 ± 0.7	0.227
Trajectory angle ($^\circ$)	=	-0.8 ± 0.2	×	Stimulus angle ($^\circ$)	+	170 ± 13	0.189
Trajectory angle ($^\circ$)	=	36 ± 6	×	Stage 2 onset (ms)	+	0.8 ± 0.3	0.392
Max. S1 velocity ($L s^{-1}$)	=	0.03 ± 0.01	×	S1 ipsi. magnitude (CVms)	+	4.7 ± 0.4	0.201
S1 contra. magnitude (CVms)	=	0.30 ± 0.03	×	S1 ipsi. magnitude (CVms)	+	$0 \pm 1^\ddagger$	0.664
S1 contra. duration (ms)	=	0.68 ± 0.05	×	S1 ipsi. duration (ms)	+	$-1 \pm 2^\ddagger$	0.746
Maximum velocity ($L s^{-1}$)	=	0.08 ± 0.01	×	S2 contra. magnitude (CVms)	+	6.3 ± 0.3	0.500

All regressions are significant with $P \leq 0.001$.

S1, stage 1; S2, stage 2; contra, contralateral.

‡ Not significantly different from 0.

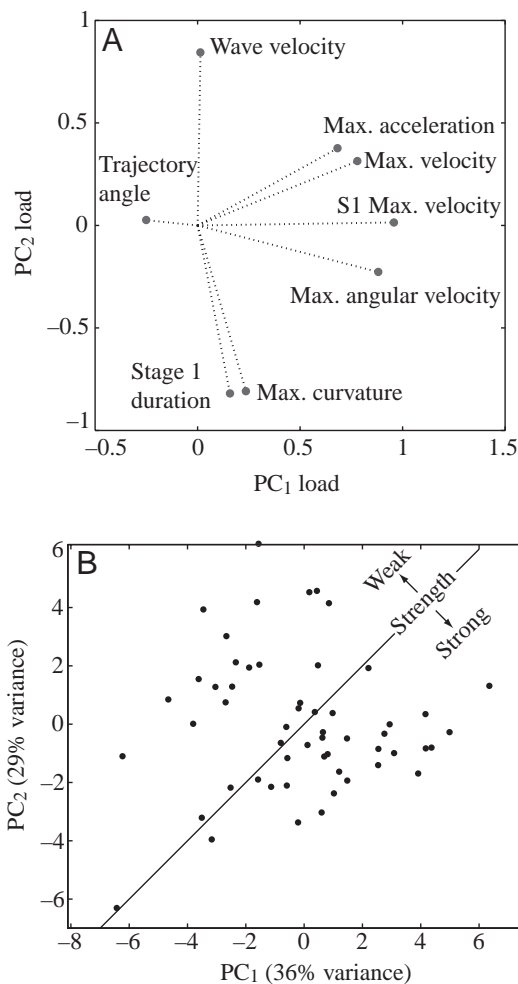


Fig. 4. Principal components analysis (PCA) on kinematic variables. (A) Principal components 1 and 2 (PC1 and PC2) loadings. Loadings are scaled so that the variance of the transformed data is the same along all axes. (B) Transformed data scores on the PC1 and PC2 axes. According to the kinematic strength metric, based on the PCA, responses with scores in the bottom right are strong, while those in the upper left are weak. The black line separates the two regions.

of the electrode on that side (five positions from anterior to posterior), and the kinematic strength of the turn. It also helps control for the effect of different individuals, which is a random factor. A four-way test was required because the variation in behavior strength tended to obscure significant effects of electrode position and side unless it was also included as an effect in the test.

Table 3 lists the results of the MANOVA, which had five significant effects: the individual, the side of the activity (I.C.), the longitudinal position of the activity (Pos.), the interaction between Pos. and the behavior's kinematic strength (Strength), and the interaction between I.C., Pos. and Strength. Univariate ANOVAs were applied only after a significant result from the MANOVA. Table 4 summarizes the results for each of the three independent variables. For all three variables, significant differences were observed between different individuals and between the ipsilateral and contralateral sides. Additionally,

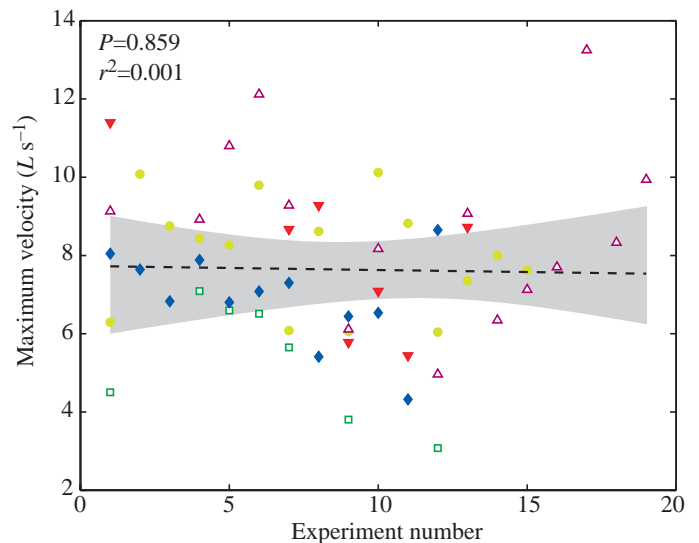


Fig. 5. Individuals did not become habituated to the stimulus. Maximum velocity ($L s^{-1}$) plotted against the experiment number in order over time. Different individuals are shown with different colors and symbol shapes. The non-significant regression is shown as a dashed line with a 95 % confidence interval in grey.

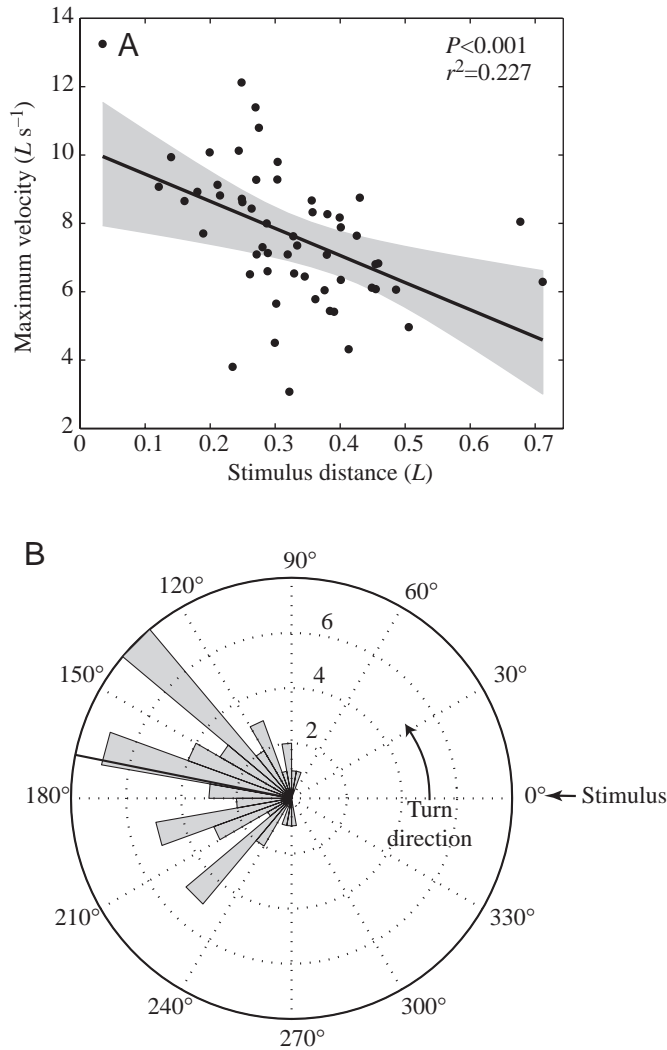


Fig. 6. Final velocity and trajectory angle are correlated with the stimulus. (A) Maximum overall velocity plotted with respect to the distance between the stimulus and the fish's center of mass. The regression line is shown in black with a 95% confidence interval in gray. (B) Angular histogram of the angle between the final trajectory and the stimulus. Angles are normalized as if all turns were to the left. The mean value of this angle is $169 \pm 6^\circ$, which is shown by the solid line. Numbers inside the circles are the frequencies of occurrence for different turn angles.

offset times and activity magnitudes varied significantly with the longitudinal position of the electrode, while magnitudes were also significantly affected by the interaction between I.C. and Strength, and that between the I.C., Pos. and Strength. The MANOVA generates a 'mean EMG pattern' for strong and weak behaviors using a standard least-squares regression, which is plotted in Fig. 8. This plot shows the overall differences between the two kinematic strengths, controlling for the variation between individuals.

Fig. 8 provides an interpretation of the significant effects in Table 3, as follows. For all behaviors, onset times are generally earlier on the ipsilateral side than the contralateral (I.C. effect; $P=0.024$), probably mostly due to the delayed onset on the

Table 3. Four-way mixed-model MANOVA on stage 1 onset and offset time and muscle activity magnitude

Effect	Pillai trace	F	d.f.	P
Individual	0.136	5.066	12, 1281	<0.001
Longitudinal position	1.065	2.201	12, 48	0.027
Ipsilateral versus contralateral	0.998	277.536	3, 2	0.004
Kinematic strength	0.934	9.469	3, 2	0.097
Pos. \times I.C.	0.902	1.721	12, 48	0.092
Pos. \times Strength	0.673	1.156	12, 48	0.341
I.C. \times Strength	1.000	3582.667	3, 2	<0.001
Pos. \times I.C. \times Strength	0.986	1.957	12, 48	0.050

$N=527$.

d.f., degrees of freedom; I.C., side of activity; Pos., longitudinal position of activity; Strength, the behavior's kinematic strength.

Significant results are shown in bold.

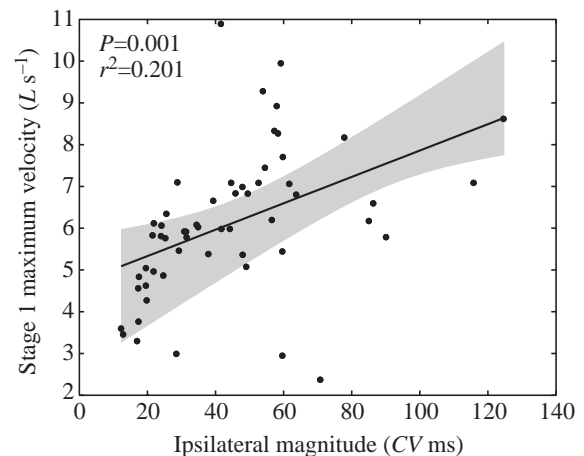


Fig. 7. Stage 1 maximum velocity correlates with ipsilateral stage 1 EMG magnitude. The linear regression line is shown in black with a 95% confidence interval in gray.

most anterior contralateral channel. Offset times are later on the ipsilateral side for all behaviors (I.C. effect; $P<0.001$); additionally, they tend to be even later in more posterior positions (Pos. effect; $P=0.002$), although more so in weak behaviors than strong. Finally, although magnitudes are always significantly greater on the ipsilateral side than the contralateral side for both behaviors (I.C. effect; $P<0.001$), the difference in magnitude between the two sides increases as the strength of the behavior increases (I.C. \times Strength effect; $P=0.003$), and the overall distribution of magnitudes from anterior to posterior and between the two sides changes for different strengths (Pos. \times I.C. \times Strength effect; $P=0.016$).

Despite the above analysis, which indicates that stage 1 ipsilateral muscle activity is longer and stronger than contralateral, the contralateral muscles still have substantial activity. To investigate the potential for increasing body wave velocity by stiffening the body, we examined the relationship of the stiffening parameter B_{EMG} to wave velocity. However, both contralateral magnitude and duration are simply a

Table 4. Four-way univariate mixed-model ANOVA results for muscle activity during Stage 1

Effect	d.f.	Magnitude (N=560)		Onset (N=527)		Offset (N=527)	
		F	P	F	P	F	P
Individual	4, *	3.938	0.004	4.745	0.001	6.794	<0.001
Longitudinal position	4, 16	3.717	0.025	0.222	0.922	6.912	0.002
Ipsi. versus contra.	1, 4	198.8	<0.001	12.432	0.024	245.6	<0.001
I.C. × Strength	1, 4	47.191	0.002	1.304	0.317	0.091	0.778
Pos. × I.C. × Strength	4, 16	4.736	0.010	0.576	0.684	1.747	0.189

Only effects that were significant in the MANOVA (Table 3) are shown here.

d.f., degrees of freedom for F test.

Significant results are shown in bold.

N values are lower for onset and offset times than for magnitude because absence of muscle activity was treated as zero magnitude, but was a missing value for onset and offset time.

* Error d.f. for magnitude, 460; for onset and offset times, 427.

Ipsi., ipsilateral; contra., contralateral. Other abbreviations as in Table 3.

constant fraction of the corresponding ipsilateral value (Fig. 9). The regressions in Fig. 9 are both significant ($P < 0.001$ in both cases) and have intercepts not significantly different from zero ($P = 0.741$ and 0.493 for Fig. 9A and B, respectively), which means that B_{EMG} is constant and equal to 1.4 ± 0.2 , based on EMG magnitudes for all responses observed. Because B_{EMG} is calculated under the assumption that muscle activity magnitude or duration are proportional to muscle force, it may not accurately describe the body stiffening. To verify the independence of bilateral activity and wave velocity, we also considered other metrics of bilateral activity, including normalized and unnormalized ratios and differences of ipsilateral and contralateral magnitude, amplitude and duration. Because contralateral activity is a constant fraction of ipsilateral (Fig. 9), all ratios and normalized differences between the two sides are constant. Unnormalized differences are proportional to the ipsilateral activity, which is not significantly correlated with wave velocity. Therefore, in the range of responses observed, no relationship between bilateral activity and wave velocity exists.

Additionally, we hypothesized that increasing wave velocity

should increase the final speed of the response. However, wave velocity showed no significant relationship with any indicator of speed ($P > 0.10$ in all cases), including maximum stage 1 and overall velocities, as well as maximum acceleration.

Stage 2

Stage 2 muscle activity was observed in almost every response: 61 out of 65 responses (94%) had at least some stage 2 activity, and 29 (45%) had stage 2 activity on all channels. In fact, having all channels active is significantly more probable than having partial or no activity (χ^2 (2 d.f.) = 21.8, $P < 0.001$). No significant correlation was found between frequency of stage 2 activity and the kinematic strength of the

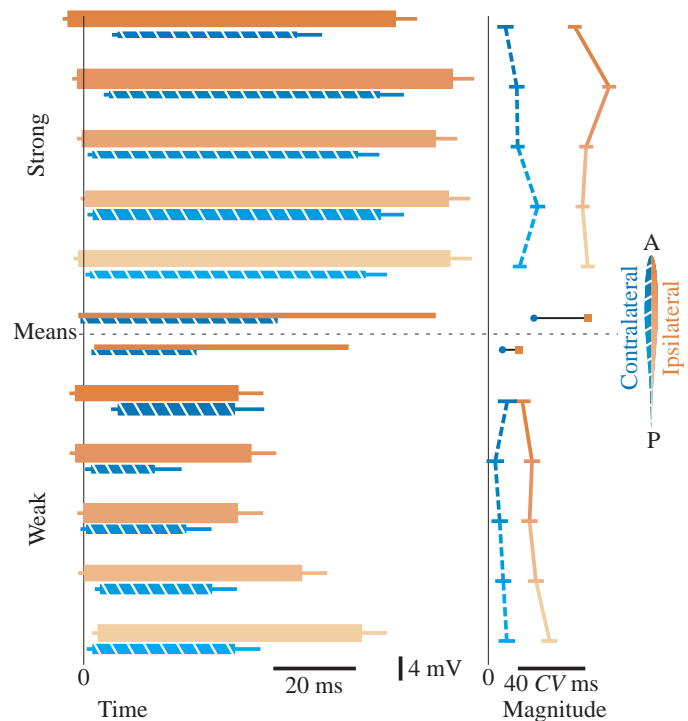


Fig. 8. Least-squares onset time, offset time and magnitude values for strong and weak escape responses, based on the MANOVA calculation (Table 3). In the left panel, mean activity is plotted against time. Different longitudinal electrode positions are displayed along the vertical axis, with anterior positions in dark colors at the top and posterior ones in light colors at the bottom. Ipsilateral and contralateral electrodes at the same longitudinal position are offset slightly from each other and are shown in orange and blue, respectively. The left and right side of the boxes are onset and offset times, respectively, and the height of each box represents the average EMG amplitude. The area of the box, thus, is proportional to the magnitude of muscle activity. The lines at either end show standard errors for the onset and offset time. The right panel shows the magnitude itself for each electrode, with standard error bars. Between the two strength responses are the means for all positions along the body of onset time, offset time and magnitude.

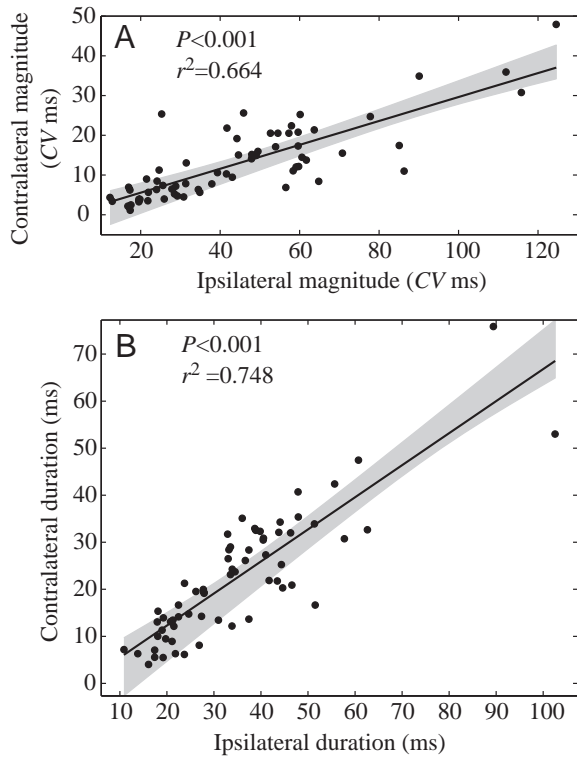


Fig. 9. Contralateral activity is significantly related to ipsilateral activity. In both plots, the regression line is shown with a 95% confidence interval in gray. (A) Regression of contralateral magnitude on ipsilateral magnitude. (B) Regression of contralateral duration on ipsilateral duration.

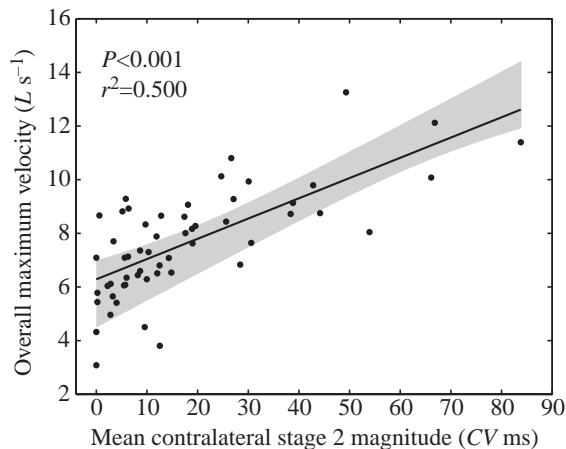


Fig. 10. Overall maximum velocity is proportional to mean contralateral stage 2 muscle activity magnitude. The linear regression line is shown in black with a 95% confidence interval in gray.

response (χ^2 (2 d.f.)=1.2, $P=0.863$), but some individuals tended to have more activity than others (χ^2 (8 d.f.)=16.3, $P=0.046$). When activity was present, it was most often seen in the two most anterior channels (homogeneity across all channels: G (4 d.f.)=25.11, $P<0.001$; homogeneity in anterior 2: G (1 d.f.)=2.76, $P=0.097$; for details of the test procedure, see Sokal and Rohlf, 1995).

Not only was stage 2 muscle activity usually present, it contributed strongly to the final escape performance. The onset time of stage 2 correlates significantly with the final trajectory angle ($P=0.001$; Table 2). The final angle ranged from 21° to 206° , with a mean of $130\pm 7^\circ$, where 0° is straight ahead for the fish. Additionally, the mean stage 2 EMG magnitude is the best predictor of the overall maximum velocity ($r^2=0.500$; Fig. 10). Although the mean stage 1 EMG magnitude correlated well with the stage 1 velocity maximum (Fig. 7, Table 2), it was not as good a predictor of the overall maximum velocity ($r^2=0.082$). The sum of mean stage 1 and stage 2 magnitude was also not as good a predictor of maximum velocity as the stage 2 magnitude alone ($r^2=0.308$). Thus, a primary determinant of the overall maximum velocity is the magnitude of stage 2 muscle activity.

Discussion

Muscle activation patterns

The kinematic strength of the escape response in *P. senegalus* is highly variable; the muscle activity patterns, however, are much like those previously described in more derived fishes (e.g. Eaton et al., 1988; Jayne and Lauder, 1993), except that the contralateral muscles are substantially active during stage 1. The variation in kinematic strength partially results from variability in stimulus strength and is controlled mechanically by a change in duration of a simple muscle activation pattern. However, it is difficult to characterize the function of the bilateral muscle activity, because body stiffening is constant over all the responses we observed. Despite these differences in stage 1, the stage 2 activity is very much like the classic pattern described in previous studies (e.g. Eaton et al., 1988; Jayne and Lauder, 1993; Foreman and Eaton, 1993).

First, the stimulus strength, gauged by the distance and angle of the object from the fish's center of mass, partially explains the variability in kinematic strength. Maximum velocity, which was generally reached during stage 2, was significantly correlated with stimulus distance (Fig. 6A). Because the correlation is low ($r^2=0.227$), other cues, such as the object's velocity, probably also contribute to the variation, but could not be measured in this study. No kinematic variable other than overall maximum velocity correlated significantly with stimulus distance.

Additionally, the final trajectory is generally in the opposite direction to the stimulus ($169\pm 6^\circ$, Fig. 6B), but not exactly 180° away. In only three cases did the fish turn less than 90° away from the stimulus. Previous studies (Eaton and Emberley, 1991; Domenici and Blake, 1993, 1997) have found coefficients lower than unity in the regression between stimulus angle and final trajectory angle, unlike what we observed in *P. senegalus*. A coefficient lower than one implies that, for some positions of a stimulus, the fish may turn away from it by varying amounts. For example, from Domenici and Blake's regression (1997), a stimulus coming from directly beside the fish (90°) would produce a turn of 141° away from

the stimulus, whereas a stimulus from directly in front of the fish (0°) would produce a turn of 91° away. *P. senegalus*, in contrast, always turns about 169° away from the stimulus, regardless of the stimulus position.

Our data tentatively suggest that the fish primarily responds to the stimulus in stage 2, about 60 ms after the stimulus was given. Both maximum velocity and final trajectory angle are functions of the stimulus intensity, and seem to be determined mechanically by stage 2 muscle activity (Table 2, Fig. 10). The maximum velocity is best predicted by stage 2 muscle activity magnitude, and the trajectory angle by the onset of that stage 2 activity; therefore, the fish seem to be modulating stage 2 activity based on the sensory information received from the stimulus prior to the onset of stage 1.

Although the sensory cues that cause variation are unclear, the mechanism is apparent: kinematic strength primarily varies according to changes in duration of the muscle activity. Fig. 8 illustrates this issue directly: the mean amplitudes of the EMGs (heights of the boxes) do not change very much, although their lengths do. More quantitatively, the EMG magnitude is the product of the mean amplitude of muscle activity, which does not vary substantially ($1.05 \pm 0.04 CV$ and $1.0 \pm 0.1 CV$, for strong and weak responses, respectively), and the duration of that activity, which approximately doubles (37 ± 1 ms and 18 ± 1 ms). In fact, neither the ipsilateral nor the contralateral amplitudes differ significantly between different strength responses (Bonferroni-corrected pairwise comparison; $P=0.184$ and $P=1.000$, respectively). The maximum stage 1 velocity, which is a large component of the kinematic strength (Fig. 4), is proportional to the stage 1 ipsilateral magnitude (Fig. 7). Therefore, most of the variation in kinematic strength actually results from changes in duration. This finding is similar to that of Foreman and Eaton (1993) in goldfish *Carassius auratus*, who found that the stage 1 angle, a measure of kinematic strength, increases with the duration of the ipsilateral EMG. In *P. senegalus*, however, we did not see the contralateral 'direction change' activity that they observed.

Secondly, the extent of bilateral Stage 1 activity is unusual for C-starts. *P. senegalus* has strong contralateral Stage 1 activity, lasting $65 \pm 3\%$ as long as the ipsilateral activity, and having an amplitude $48 \pm 6\%$ as large. This activity is quantitatively different from the stage 1 contralateral activity observed in goldfish *Carassius auratus* (Eaton et al., 1988; Foreman and Eaton, 1993; Zottoli et al., 1999), and bluegill sunfish *Lepomis macrochirus* (Jayne and Lauder, 1993). In both these fishes, the contralateral EMG often shows a small spike at the same time as the Mauthner impulse on the ipsilateral side. The contralateral spike may be at least partially due to volume conduction (cross talk) from the ipsilateral side (Zottoli, 1977; Eaton et al., 1988; Foreman and Eaton, 1993). If it does represent any true muscular contraction, it is quite different from the contralateral activity we observed in *P. senegalus*; contralateral activity in *C. auratus* and *L. macrochirus* begins at the same time as the ipsilateral activity, but lasts for a much shorter time (<15% of the ipsilateral duration in *L. macrochirus*). Of the species identified by Hale et al. (2002) as

having bilateral stage 1 activity, only the bowfin, *Amia calva*, seems to show it to the same extent as *P. senegalus*.

Not only is the strong contralateral stage 1 activity unusual, it does not seem to have the expected function of modulating wave speed or escape speed. Long and colleagues (Long et al., 1994; McHenry et al., 1995; Long and Nipper, 1996; Long, 1998) have explored the effects of body stiffness in various fishes and have consistently found that increasing flexural stiffness increases body wave speed. Their studies only examined unilateral contralateral activity and imposed an external bending moment, which may be equivalent to the ipsilateral muscle contraction in this study. With the appropriate contralateral phase relative to the external bending, the effective body stiffness changes, changing the body's resonant frequency. Propagating a wave at a frequency close to the resonant frequency often takes dramatically less energy than at other frequencies (Marion and Thornton, 1995; Long, 1998); thus, changing the resonant frequency will tend to change the body wave velocity.

On the basis of their findings, we hypothesized that the bilateral contraction observed should increase the body stiffness, thus increasing the body wave velocity. In particular, we expected that the higher the B_{EMG} value, the stiffer the body would be and the faster the wave would be. This might seem contradictory; the bilateral activity occurs during stage 1 and the body wave propagates mostly during stage 2. However, the two do overlap substantially. The wave begins traveling at 16.2 ± 0.2 ms, independent of the strength of the response or the wave speed, while stage 1 muscle activity lasts 29 ± 1 ms on average. Thus, the two overlap by about 13 ms, 45% of time in which bilateral activity and, hence body stiffening, is occurring. Muscle takes time to relax after the end of the EMG signal (Lieber, 1992), so the overlap may actually be longer than the measured 13 ms. Even if bilateral activity is capable of increasing wave speed, for all the responses we observed, the magnitude and duration of contralateral activity were a constant multiple of the corresponding ipsilateral value (Fig. 9), meaning that the B_{EMG} value was approximately constant. Because B_{EMG} is calculated under the uncertain assumption that EMG activity is proportional to muscle force, we also tested other metrics for bilateral activity. Wave velocity was not correlated with any metric of bilateral activity. Therefore, if bilateral activity in *P. senegalus* does cause an increase in body wave velocity, it does it by a constant amount for all the responses we observed.

It is not clear that bilateral activity should actually increase escape response performance. For steady swimming, body wave speed should be correlated with swimming velocity and efficiency. If the Froude efficiency remains the same, an increase in body wave speed should increase swimming velocity (Lighthill, 1970). If the Froude efficiency changes, though, wave speed may not be correlated with swimming velocity; our data show no significant correlation between the two. Indeed, increasing body wave speed by bilateral muscle contraction may actually decrease the overall efficiency, because the contralateral muscles are lengthening while active

and thus producing negative work. Even though muscles produce negative work more efficiently than positive (Lieber, 1992), the total muscular work would still be reduced. Even so, if the tuning of body stiffness results in a body wave traveling at closer to the body's resonant frequency, the mechanical cost to produce that wave could be substantially lower. Depending on the relative magnitude of muscle energy input to produce the body wave energy output, the efficiency could increase or decrease. Additionally, bilateral activity also changes the torque exerted by the axial musculature on the spine. Longitudinal variations in muscle torque resulting from the contralateral contraction could also increase or decrease the bending wave velocity (Wakeling and Johnston, 1999).

Finally, although the high variability and strong contralateral muscle activity are unusual in C-starts, the stage 2 pattern is typical of C-starts in other fishes (e.g. Eaton et al., 1988; Jayne and Lauder, 1993). In 94% of analyzed responses, there was some muscle activity during stage 2, propagating in a wave down the body. The data we collected differ primarily in this respect from those of Westneat et al. (1998), who observed little stage 2 activity. Their contralateral electrode was positioned close to the fish's center of mass, corresponding to a position slightly posterior of our site 2 (Fig. 1). Our results show that stage 2 activity is strongest and most frequent at the first two sites, which they might not have observed, due to their electrode position. Even so, they did note some activity in a third of the cases in their anterior electrode, similar to the pattern we observed. In general, we find that escape responses in *P. senegalus* have stage 2 contralateral muscle activity, but primarily in the anterior third of the body.

Not only is there usually stage 2 muscle activity, but its magnitude primarily determines the final velocity. In the absence of muscle activity, a stage 2 kick could still exist, due to passive straightening of the body (Johnsrude and Webb, 1985; Eaton et al., 1988; Foreman and Eaton, 1993). Although this passive straightening may have some effect, the final velocity in the C-start is significantly related to the magnitude of the stage 2 muscle activity (Fig. 10), indicating that the main force for the kick is coming from active muscular contraction.

Implications for reticulospinal control

Our data support the hypothesis that the escape response, although initiated by Mauthner cells, is controlled by a more complex circuit (Eaton et al., 1988; Eaton and Emberley, 1991; Foreman and Eaton, 1993; Zottoli et al., 1999), because we observed substantial variation among startle responses. Direct stimulus of a Mauthner cell produces a stage 1 response with a fairly constant duration and final trajectory angle (Nissanov and Eaton, 1989); more variation thus indicates that other neurons may be involved in the sensory response. Other neurons are indeed responsible for aspects of the escape response: descending interneurons that are active during escape responses have been identified (Fetcho, 1992) and escape responses are possible, though less likely, when Mauthner cells have been ablated (Zottoli et al., 1999) or do not exist (Hale, 2000). We observed an almost tenfold variation

in stage 1 duration, corresponding to large variability in maximum velocity and final trajectory angle, similar to what Foreman and Eaton (1993) observed. The Mauthner cells alone are unlikely to be able to produce such a range. The variation in our stimulus strength also supports this conclusion, because a simple circuit, like Nissanov and Eaton (1989) examined, should produce an 'on-off' type of behavior, in which the strength of the behavior does not vary with stimulus strength. Because the behavior did change for the range of stimuli, there must be neurons that modulate the response based on the strength of the sensory input.

The strong bilateral activity may not substantially increase the escape response circuit's complexity, because the contralateral duration and magnitude are simply constant fractions of the ipsilateral activity (Fig. 9). Therefore, the escape response in *P. senegalus* is probably mediated by a more complex circuit than just the Mauthner cell, but not one requiring substantially more complexity than in fishes without bilateral activity.

With such strong bilateral activity, it is somewhat surprising that *P. senegalus* performs a true C-start. Several previous studies have found that bilateral activity in some elongate fishes causes a head-retraction behavior, in which the head is withdrawn in an accordion-like motion (Currie and Carlsen, 1987; A. B. Ward, personal communication). Fishes that do head retraction rather than C-starts seem to lack an axon cap, a structure that prevents simultaneous firing of both Mauthner cells (Meyers et al., 1998). *P. senegalus*, though an elongate fish, has a 'primitive' axon cap, lacking visible divisions into central and peripheral portions (Stefanelli, 1980). Our data suggest that its axon cap provides partial inhibition of activity on the contralateral side. Partial inhibition seems sufficient to generate a typical C-type escape response, however, because no head withdrawal behavior was ever observed.

In conclusion, we confirm that the bilateral stage 1 activity in *P. senegalus* is the primary difference between its escape response and those of more derived actinopterygians, as previously demonstrated (Westneat et al., 1998). *P. senegalus* shows both stage 1 and stage 2 activity. Although responses vary greatly in overall strength, the variation is controlled by changes in stage 1 muscle activity duration, as previously observed in goldfish, *Carassius auratus* (Foreman and Eaton, 1993). Bilateral activity in *P. senegalus* may stiffen its body, but it does so by a constant amount over the variation we observed; therefore, it does not modulate fast-start wave speed by changing body stiffness. Additionally, *P. senegalus* has substantially stronger contralateral stage 1 activity than has been observed in any more derived actinopterygian. Future comparisons between its behavior and the derived C-start pattern may help to provide insight into the evolution of Mauthner cells, the escape response behavior, and its modification in elongate fishes.

We would like to thank Jennifer Nauen, Jimmy Liao, Andie Ward, Manny Assizi, Mark Westneat and Melina Hale for helpful commentary on the manuscript. Two anonymous

referees also helped improve the manuscript. Steven Zottoli provided a useful reference on axon cap structure in *Polypterus*. Support was provided by NSF grant 9807021 to G.V.L.

References

- Beer, F. P. and Johnston, E. R.** (1992). *Mechanics of Materials*. 2nd edition. New York: McGraw-Hill.
- Currie, S.** (1984). Mauthner cells, Müller cells, and the lamprey startle response. *Biol. Bull.* **167**, 525.
- Currie, S. and Carlsen, R. C.** (1987). Functional significance and neural basis of larval lamprey startle behavior. *J. Exp. Biol.* **133**, 121–135.
- Domenici, P. and Blake, R. W.** (1993). Escape trajectories in angelfish (*Pterophyllum eimekei*). *J. Exp. Biol.* **177**, 253–272.
- Domenici, P. and Blake, R. W.** (1997). The kinematics and performance of fish fast-start swimming. *J. Exp. Biol.* **200**, 1165–1178.
- Domenici, P. and Blake, R. W.** (1991). The kinematics and performance of the escape response in the angelfish (*Pterophyllum eimekei*). *J. Exp. Biol.* **156**, 187–205.
- Dunteman, G. H.** (1989). *Principal Components Analysis*. Newbury Park, CA: SAGE Publications.
- Eaton, R. C., DiDomenico, R. and Nissanov, J.** (1991). Role of the Mauthner cell in sensorimotor integration by the brain stem escape response. *Brain Behav. Evol.* **37**, 272–285.
- Eaton, R. C., DiDomenico, R. and Nissanov, J.** (1988). Flexible body dynamics of the goldfish C-start: Implications for reticulospinal command mechanisms. *J. Neurosci.* **8**, 2758–2768.
- Eaton, R. C. and Emberley, D. S.** (1991). How stimulus direction determines the trajectory of the Mauthner-initiated escape response in a teleost fish. *J. Exp. Biol.* **161**, 469–487.
- Ellerby, D. J. and Altringham, J. D.** (2001). Spatial variation in fast muscle function of the rainbow trout *Oncorhynchus mykiss* during fast-starts and sprinting. *J. Exp. Biol.* **204**, 2239–2250.
- Fetcho, J. R.** (1991). Spinal network of the Mauthner cell. *Brain Behav. Evol.* **37**, 298–316.
- Fetcho, J. R.** (1992). Excitation of motoneurons by the Mauthner axon in goldfish: Complexities in a 'simple' reticulospinal pathway. *J. Neurophys.* **67**, 1574–1586.
- Foreman, M. B. and Eaton, J. K.** (1993). The direction change concept for reticulospinal control of goldfish escape. *J. Neurosci.* **13**, 4101–4113.
- Hale, M. E.** (2000). Startle responses of fish without Mauthner neurons: Escape behavior of the lumpfish (*Cyclopterus lumpus*). *Biol. Bull.* **199**, 180–182.
- Hale, M. E., Long, J. H., McHenry, M. J. and Westneat, M. W.** (2002). Evolution of behavior and neural control of the fast-start escape response. *Evolution* **56**, 993–1007.
- Jayne, B. C. and Lauder, G. V.** (1993). Red and white muscle activity and kinematics of the escape response of the bluegill sunfish during swimming. *J. Comp. Physiol. A* **173**, 495–508.
- Johnsrude, C. L. and Webb, P. W.** (1985). Mechanical properties of the myotomal musculo-skeletal system of rainbow trout, *Salmo gairdneri*. *J. Exp. Biol.* **119**, 71–83.
- Kaiser, H. F.** (1960). The application of electronic computers to factor analysis. *Educ. Psych. Meas.* **20**, 141–151.
- Lieber, R. L.** (1992). *Skeletal Muscle Structure and Function*. Baltimore: Williams and Wilkins.
- Lighthill, M. J.** (1970). Aquatic animal propulsion of high hydromechanical efficiency. *J. Fluid Mech.* **44**, 265–301.
- Loeb, G. E. and Gans, C.** (1986). *Electromyography for Experimentalists*. Chicago: University of Chicago Press.
- Long, J. H.** (1998). Muscles, elastic energy, and the dynamics of body stiffness in swimming eels. *Amer. Zool.* **38**, 771–792.
- Long, J. H., McHenry, M. J. and Boetticher, N. C.** (1994). Undulatory swimming: How traveling waves are produced and modulated in sunfish (*Lepomis gibbosus*). *J. Exp. Biol.* **192**, 192–145.
- Long, J. H. and Nipper, K. S.** (1996). The importance of body stiffness in undulatory propulsion. *Amer. Zool.* **36**, 678–694.
- Marion, J. B. and Thornton, S. T.** (1995). *Classical Dynamics of Particles and Systems*. 4th edition. Fort Worth: Harcourt Brace.
- McHenry, M. J., Pell, C. A. and Long, J. H.** (1995). Mechanical control of swimming speed: stiffness and axial wave for in undulating fish models. *J. Exp. Biol.* **198**, 2293–2305.
- Meyers, J. R., Copanas, E. H. and Zottoli, S. J.** (1998). Comparison of fast startle responses between two elongate bony fish with an anguilliform type of locomotion and the implications for the underlying neuronal basis of escape behavior. *Brain Behav. Evol.* **52**, 7–22.
- Nissanov, J. and Eaton, R. C.** (1989). Reticulospinal control of rapid escape turning maneuvers in fishes. *Amer. Zool.* **29**, 103–121.
- Rice, J. A.** (1995). *Mathematical Statistics and Data Analysis*. 2nd edition. Belmont, CA: Wadsworth.
- Sokal, R. R. and Rohlf, F. J.** (1995). *Biometry: The Principles and Practice of Statistics in Biological Research*. 3rd edition. New York: Freeman.
- Stefanelli, A.** (1980). I neuroni di Mauthner degli Ittiopsidi. Valutazioni comparative morfologiche e funzionali. *Lincei Mem. Sci. Fis. Natur. Ser. VIII, Vol. XVI*, 1–45.
- Taylor, J. R.** (1982). *An Introduction to Error Analysis*. Sausalito, CA: University Science Books.
- Wakeling, J. M. and Johnston, I. A.** (1999). Body bending during fast-starts in fish can be explained in terms of muscle torque and hydrodynamic resistance. *J. Exp. Biol.* **202**, 675–682.
- Walker, J. A.** (1998). Estimating velocities and accelerations of animal locomotion: A simulation experiment comparing numerical differentiation algorithms. *J. Exp. Biol.* **201**, 981–995.
- Webb, P. W.** (1978). Fast-start performance and body form in seven species of teleost fish. *J. Exp. Biol.* **74**, 211–216.
- Webb, P. W.** (1983). Speed, acceleration and manoeuvrability of two teleost fishes. *J. Exp. Biol.* **102**, 115–122.
- Weih, D.** (1972). A hydrodynamical analysis of fish turning manoeuvres. *Proc. R. Soc. Lond. B* **182**, 59–72.
- Westneat, M. W., Hale, M. E., McHenry, M. J. and Long, J. H.** (1998). Mechanics of the fast-start: Muscle function and the role of intramuscular pressure in the escape behavior of *Amia calva* and *Polypterus palmas*. *J. Exp. Biol.* **201**, 3041–3055.
- Zar, J. H.** (1999). *Biostatistical Analysis*. 4th edition. Upper Saddle River, NJ: Prentice Hall.
- Zottoli, S. J.** (1977). Correlation of the startle reflex and Mauthner cell auditory responses in unrestrained goldfish. *J. Exp. Biol.* **66**, 243–254.
- Zottoli, S. J., Newman, B. C., Rieff, H. I. and Winters, D. C.** (1999). Decrease in occurrence of fast startle responses after selective Mauthner cell ablation in goldfish (*Carassius auratus*). *J. Comp. Physiol. A* **184**, 207–218.